Clogging: bridge formation and vibration-based destabilization

Julio R. Valdes and J. Carlos Santamarina

Abstract: The migration of mobile particles through porous networks is restricted when the size of the migrating particles approaches the size of pore throats. In this case, single particle retention or entrapment by bridge formation takes place. Experimental results show that bridge formation and stability are controlled by particle shape, relative throat-to-particle size, and skeletal forces. Forced-vibration studies provide additional insight into bridge stability and the potential for vibration-based unclogging, and show that it is easier to prevent bridge formation than to destabilize already formed bridges. Results from these pore-scale studies are relevant to filter clogging and unclogging, water and oil extraction, sand production in oil wells, and in food grain, aggregate and powder handling operations.

Key words: filters, bridging, clogging, particles, vibration, unclogging.

Résumé : La migration de particules mobiles à travers des réseaux poreux est limitée lorsque la dimension des particules migrantes s'approche de la dimension des collets des pores. Dans ce cas, la retenue de particules simples ou le piégeage par la formation de ponts se produisent. Les résultats expérimentaux montrent que la formation de ponts et la stabilité sont contrôlées par la forme des particules, la dimension relative des particules et des collets des pores, et les forces du squelette. Des études avec des vibrations forcées fournissent un éclairage additionnel sur la stabilité des ponts et le potentiel de déblocage par les vibrations, et montrent qu'il est plus facile de prévenir la formation de ponts que de déstabiliser les ponts déjà formés. Les résultats de ces études à l'échelle des pores sont pertinents au colmatage et déblocage des filtres, à l'extraction de l'eau et de l'huile, à la production de sable dans les puits d'huile, et aux opérations de manipulation de grains d'aliments, d'agrégats et de poudres.

Mots-clés : filtres, formation de ponts, colmatage, particules, vibration, déblocage.

[Traduit par la Rédaction]

Introduction

Filtration takes place when a porous network, such as a soil mass, captures migratory particles within its pore structure. Single migratory particles are retained at small pore throats and remain inside pore chambers. Particle entrapment can also occur when migrating particles with size d form bridges at pore throats with size d_o that are larger than the migratory particles, that is, $d_o/d > 1$ (U.S. Corps of Engineers, Waterways Experiment Station WES 1953; Sakthivadivel and Einstein 1970; Ives 1980; Gruesbeck and Collins 1982; McDowell-Boyer et al. 1986; Ramachandran and Fogler 1999; Watson and John 1999). It is anticipated that the likelihood of bridging decreases as d_o/d increases. Figure 1 depicts the different regimes for particle entrapment.

The purpose of this study is to investigate the pore-scale mechanisms involved in bridge formation and destabilization. The scope is limited to large migrating particles, so that electrical forces are significantly smaller than particle self-weight, to dry systems that are not affected by fluid flow, and to flat circular orifices. Experimental procedures, results, and analyses follow. Details of the study and the complete dataset can be found in Valdes (2002). The complementary macroscale study of fines migration and clogging during fluid flow is documented in Valdes and Santamarina (2006).

Received 1 September 2006. Accepted 19 September 2007. Published on the NRC Research Press Web site at cgj.nrc.ca on 5 March 2008.

J.R. Valdes.[1] Department of Civil and Environmental Engineering, San Diego State University, 5500 Campanile Drive, San Diego, CA 92182, USA.
J.C. Santamarina. School of Civil and Environmental Engineering, Georgia Institute of Technology, 790 Atlantic Drive, Atlanta, GA 30332, USA.

[1]Corresponding author (e-mail: jvaldes@mail.sdsu.edu).

Bridge formation

The formation of granular bridges is explored first. Emphasis is placed on the influence of particle shape on the maximum throat-to-particle size ratio d_o/d for which bridging is attainable.

Bridging and particle shape – experimental study

This experimental study is designed to gain insight into bridge formation starting from a stable packing. Three different particle types are selected: glass beads (smooth spherical), Ottawa sand (quasismooth, not angular), and mica flakes (platy); particle characteristics are summarized in Table 1. The experimental device consists of an acrylic tube placed on top of a plate that has a central orifice of diameter d_o; the orifice represents the pore throat (Fig. 2*a*). With the orifice closed, the tube is filled with the selected particles to a predetermined height. The plug closing the orifice is then removed to allow particle passage through the orifice. The test was repeated for various orifice sizes to determine bridging and passing regimes.

 doi:10.1139/T07-088

Fig. 1. Regimes for particle bridging. Particles of size d and throats of size d_o. The boundary between bridging and no entrapment is sought in this study.

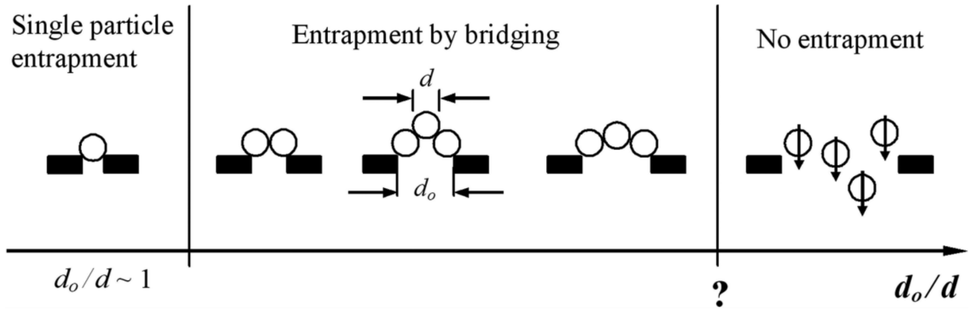

Table 1. Particles selected for the experimental study.

Particles	Photo	Shape	G_s^a	d_{50} (mm)	C_u^b
Glass beads		Smooth spherical ($R = 0.95$, $S = 0.95$)[c]	2.65	0.65	1.0
Ottawa sand	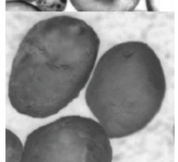	Quasi-smooth not angular ($R = 0.9$, $S = 0.8$)[c]	2.65	0.72	1.25
Mica[d]	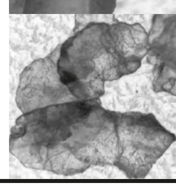	Smooth platy	2.67	Width ~ 1 Length ~ 1 Thickness ~ 0.12	2.27

[a] G_s, specific gravity.
[b] C_u, coefficient of uniformity, equal to d_{60}/d_{10}.
[c] Sphericity S and roundness R values obtained using chart in Krumbein and Sloss (1963).
[d] Mica size obtained through sieving and microscopy observations.

Results in Fig. 3 show that characteristic bridging thresholds $\delta = d_o/d$ depend on particle sphericity, roundness, and surface roughness. Three regimes are identified: stable bridge formation occurs when $d_o/d < \delta_{min}$, intermittent bridge formation and destabilization events occur when $\delta_{min} < d_o/d < \delta_{max}$, and no bridging is observed when $d_o/d > \delta_{max}$. In the intermittent regime ($\delta_{min} < d_o/d < \delta_{max}$), bridge stability is notably sensitive to external vibrations, suggesting that vibration-based techniques can prove useful for unclogging porous media by promoting the destabilization of bridges in this relative size regime. Note that smooth and spherical glass beads form smaller bridges in both regimes.

The detailed observation of bridges formed by mica particles reveals two distinct structures (Fig. 3). At low d_o/d ratios, mica platelets align parallel to the base plate and readily plug the orifice, disallowing particle flow (note that $d = 1$ mm for mica according to Table 1). However, as the d_o/d ratio approaches the intermittent regime, bridges are formed by flowing particles that are aligned towards the orifice. The intermittent regime for flat particles is probably dependent on the shape of the throat due to the inherent particle alignment exhibited by flat particles; however, this hypothesis has not been experimentally confirmed.

The orifice diameter d_o can be related to the equivalent circular pore throat in a granular filter. Consider a filter made of monosized particles of diameter D. The ratio between the particle size and the pore throat size is $D/d_o = 2.41$ for a simple cubic packing and $D/d_o = 6.5$ for a cubic tetrahedral dense packing (Fig. 4). Then, these pore-scale results provide support to empirical filter relations, which are typically expressed in terms of $D/d = (d_o/d)(D/d_o)$, where d_o/d is obtained from Fig. 3 and the D/d_o range is identified above (refer to Bertram 1940; Sherard et al. 1984; Kenney et al. 1985; Bigno et al. 1994).

Force chains (photoelasticity)

Particulate bridges are seldom smooth geometric arches subjected to homogeneous confining forces. Instead, preliminary observations reveal that the stability of a bridge is strongly influenced by its geometry and the distribution of contact forces within the granular medium.

Fig. 2. Devices and peripherals used for the experimental studies. (*a*) Bridge formation. (*b*) Bridge destabilization.

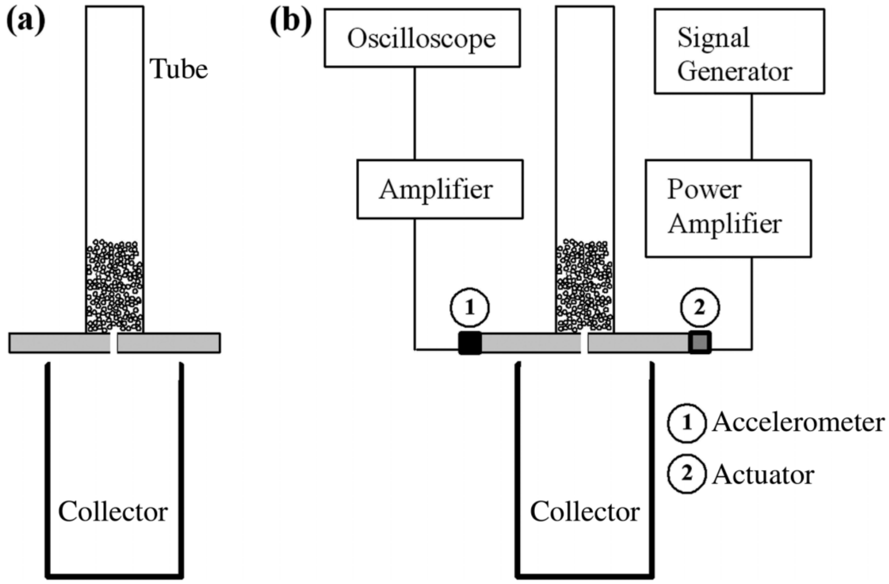

Fig. 3. Effect of particle shape on the formation of bridges spanning orifices of diameter d_o. Open circles define the "bridging regime" in Fig. 1. Filled circles denote the transition regime, where the stability of bridges is vibration sensitive. Diamonds denote the "no entrapment" regime. Particle characteristics are summarized in Table 1.

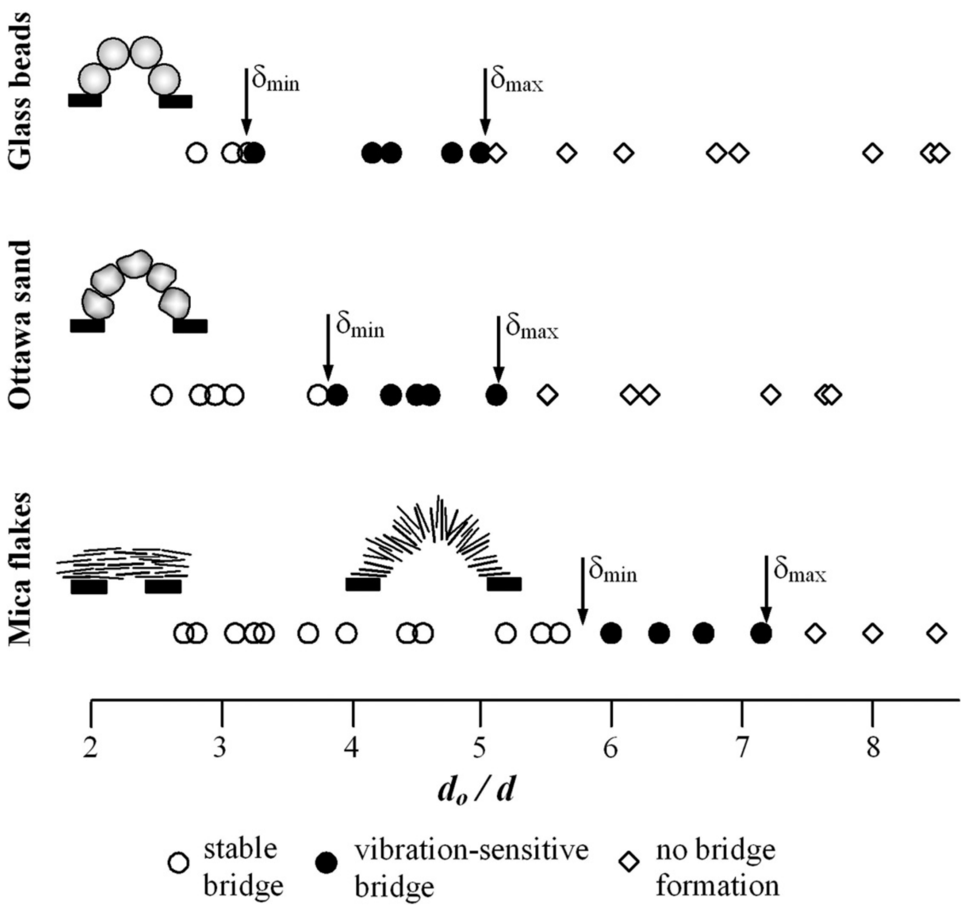

Forces are transferred through granular assemblages along networks that involve a relatively small number of particles. These preferential force paths are called force chains. The development of force chains within particle assemblages during bridge formation is studied herein using photoelasticity. Photoelastic disks are placed between two parallel acrylic sheets and polarizers. The granular skeleton is then uniformly loaded at the top of the assemblage. Base blocks are

Fig. 4. Relationship between particle size and throat size for simple cubic and tetrahedral packings.

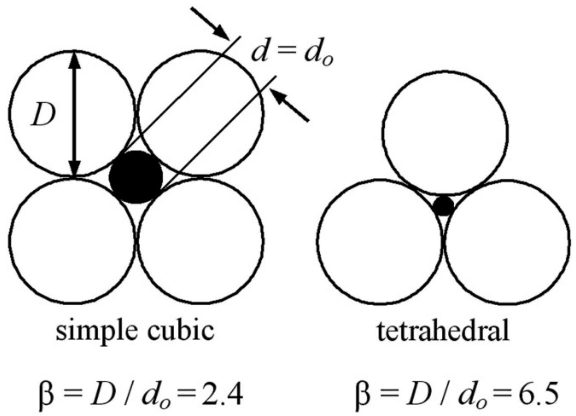

removed one by one and fringes are recorded with digital photography. Figure 5 presents an interpreted sequence of images. The following observations summarize this study (more than 30 similar tests):

- Bridge sizes can reach d_o/d = 5 in this two-dimensional system.
- The initial force chains in the far field of the bridge remain as the blocks are removed and the bridge forms. That is, force changes are local to the disturbance.
- Chains near the bridge experience major force redistribution and progressive force concentration. The most loaded force chains do not necessarily involve the exposed particles in the bridge.
- The removal of blocks that support major force chains causes significant force redistribution. In such cases, unequal shear and normal contact forces are induced within bridge particles and may cause localized slippage and bridge destabilization.

Particle-level analyses

Bridge formation involves particle shape, the mobilization of interparticle friction, and the formation of force chains within and around the granular skeleton of the bridge. The magnitude and direction of the contact forces within the particles that form the bridge are intimately related to the geometry of the bridge. Furthermore, the larger the bridge span d_o/d, the higher the regularity in the bridge geometry that is required to maintain stability.

Consider a two-dimensional circular bridge made of n spherical particles of diameter d, spanning an orifice of size d_o. The particles in the bridge are centered along the circumference of radius R, such that the angle between two adjacent particles is γ (see inset in Fig. 6). The geometrical analysis of this configuration permits deriving an expression that relates the size ratio d_o/d, the interparticle angle γ, and the number of particles n in the bridge

$$[1] \qquad \frac{d_o}{d} = \frac{\sin\left(\frac{n\pi - n\gamma}{2}\right)}{\cos\left(\frac{\gamma}{2}\right)} \qquad \gamma < \pi$$

Figure 6 shows the variation in γ as a function of d_o/d for bridges that consist of various numbers of particles n. Clearly, bridges can involve different number of particles

Fig. 5. Bridge formation and development of force chains from photoelasticity studies (interpreted from photographs in Valdes 2002). Major force chains are shown; thicknesses denote intensity. The same two particles are shaded in each sketch for reference. Bridge formation and force redistribution occur as supporting blocks are removed one by one.

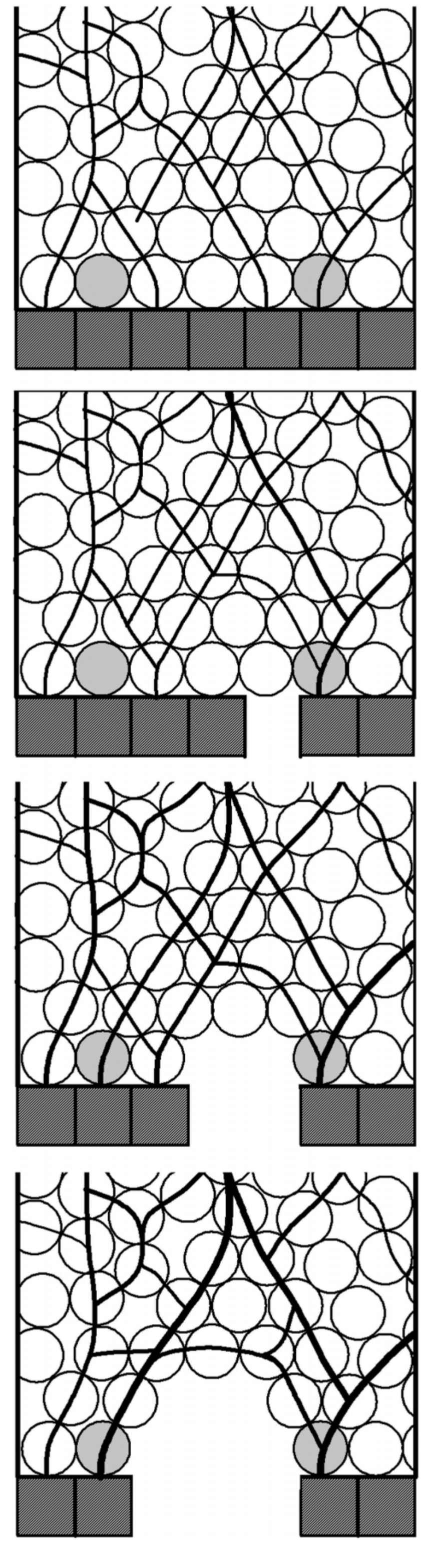

Fig. 6. Orifice-to-particle size ratio d_o/d versus interparticle angle γ for circular bridges made of n particles – two-dimensional analysis. Sketches A and B show the geometric configuration for two admissible bridges; the lower tangential boundary is given by eq. [2].

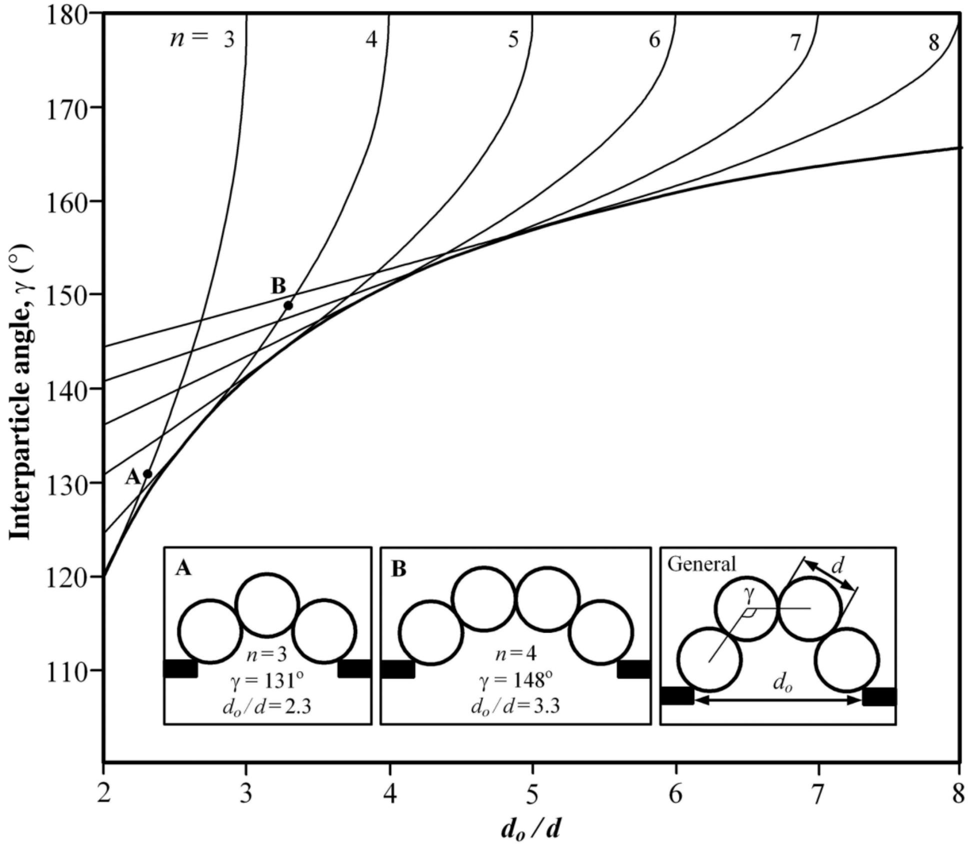

for a given d_o/d ratio. However, experimental data show that bridges made of rotund particles with d_o/d greater than 4 to 5 are unstable (i.e., vibration sensitive; Fig. 3). This suggests that deviations from a regular geometric bridge configuration leads to kinematic instabilities.

The tangent to the circular arc and the edge of the throat form an angle φ_d that is related to the interparticle angle γ and the ratio d/d_o (Fig. 7)

$$\frac{d_o}{d} = \frac{\cos(\varphi_d)}{\cos\left(\frac{\gamma}{2}\right)} \quad [2]$$

When φ_d = 0, particles within the bridge align along a semicircle that ends normal to the base so that minimal frictional resistance or lateral restraint from neighboring particles need be mobilized. Equation [2] evaluated with φ_d = 0 defines the lower tangential boundary for the trends shown in Fig. 6.

Bridge destabilization

The entrapment of migratory particles at pore throats leads to clogging of the porous medium and a severe reduction in permeability. Some geomechanics processes are hampered by clogging (e.g., oil production, water extraction, and general drainage applications); in those cases, bridge destabilization and migratory particle throughput is preferred. The experimental investigation presented next is designed to gain insight into the viability of using vibration to destabilize bridges and to hinder further bridge formation. In turn, this

Fig. 7. Boundary condition and bridge formation.

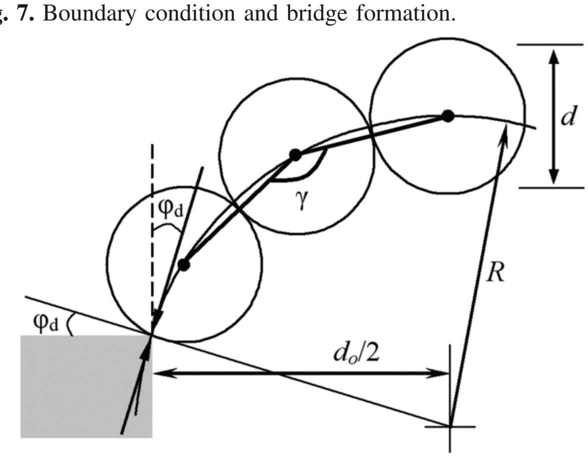

would facilitate migratory particle transport and hamper clogging.

Forced vibration effects – experimental study

The tube–orifice device used in the previous study is modified to apply controlled forced vibration onto the orifice plate (only) via a mechanical actuator fed by a sinusoidal signal generator (Fig. 2*b*). The orifice size is selected in the middle of the vibration-sensitive regime (refer to Fig. 3): d_o/d = 4.15 for glass beads and d_o/d = 4.5 for sand particles. For mica flakes, a ratio closer to the stable regime d_o/d = 5.5 is selected because larger mica flake bridges are extremely sensitive and bridge reformation after destabilization is uncommon, even in the absence of vibrations. The tube is filled with a predetermined amount of particles, and the particulate bridge forms over the orifice; the plate is then vibrated either perpendicular or parallel to the orifice axis, and its motion is monitored with an accelerometer. The system resonance is observed at around 240 Hz (filled tube – similar for both excitation directions).

Two test procedures are implemented. The first procedure involves "increasing the amplitude" of the applied signal while maintaining a constant frequency. For each frequency and amplitude condition, particle "bridging" or "passing" is observed for 60 s; in cases where granular flow through the orifice occurs intermittently, an additional 60 s are allowed after any spontaneous throughput of particles. The second procedure involves "increasing the frequency" at a constant output amplitude until a passing condition is obtained; this test sequence is performed to confirm destabilization conditions observed with the first procedure.

The measured vibration at the orifice is plotted in a tripartite plot format where the orifice acceleration a, velocity $v = a/f$, and displacement $u = a/f^2$ are shown versus frequency f to facilitate interpretation. Each plot combines the data gathered with the two test procedures, for each material and vibration direction. The resulting six plots are shown in Fig. 8. Each data point is a measurement. Crosses and circles depict bridging and passing cases, respectively, from the "increasing amplitude" procedure. Data from the "increasing frequency" procedure are shown as triangles and define a boundary between bridging and passing. Note that passes for the "increasing amplitude" procedure (circles) are clustered near resonance; however, the boundary between bridging and passing (triangles) reveals trends for a wider frequency range. (Note: a proper comparison of results gathered with different particles must take into consideration the characteristics of particle motion and the selected d_o/d ratio in relation to the values of δ_{min} previously identified for each material.) Figure 8 indicates that:

- Both test procedures define similar bridging–passing regions for each vibration direction. The bridge versus pass boundaries are relatively parallel to the acceleration axes in all cases. This suggests that acceleration is the governing parameter for bridge destabilization. (Note: the destabilizing acceleration shows a decreasing trend with increasing frequency in most cases.)
- The acceleration required to destabilize glass bead bridges is smaller than that required to destabilize sand bridges. It is hypothesized that surface roughness requires higher interparticle displacement to allow destabilization.
- Bridge regeneration is unusual once particles start flowing through the orifice after destabilization. However, the passage process appears to be affected by particle shape: sand passes are sporadic (i.e., bridges form and collapse intermittently), whereas glass beads and mica particles flow smoothly through the orifice. In addition, bridge regeneration does not occur even if the excitation frequency is lowered during the test. This suggests that vibrations may be more efficient to prevent bridging than to remediate a clogged network.
- In general, the vertical accelerations required to destabilize glass bead and sand bridges are lower than the transverse accelerations (Figs. 8*a* and 8*b* versus Figs. 8*d* and 8*e*). Mica bridges appear to be equally susceptible to transverse and vertical vibrations (Figs. 8*c* and 8*f*).

Particle-level destabilization study

High-speed photographic studies are conducted to establish the collapse mechanism of a two-dimensional bridge made of circular disks upon the application of a dynamic transverse excitation at the base of the bridge (pendulum impact loading – Fig. 9). The base plate rests on ball bearings for easy sliding. Circular bridges with d_o/d = 3 and 4, and n = 6 are formed. The assemblage is confined by rigid vertical lateral walls not anchored on the base plate, and loaded uniformly at the top, much like in the photoelasticity configuration described previously. The progression of bridge collapse after impact is digitally recorded and analyzed by slow motion replay. A total of 14 different tests were repeated for similar configurations.

Figure 9 shows a typical bridge collapse sequence. Bridges fail on the opposite side of the applied compressive disturbance, and particles-5 and -6 are the first to fall in most cases. Collapse may also start wherever there is a sequence of adjacent particles with large interparticle angle γ (i.e., poor bridge regularity). In addition, it is observed that the acceleration of particles during collapse is associated with the magnitude of the internal forces.

Two events co-exist at the onset of the plate's acceleration: (*i*) a compression front propagates from particle-1 towards particle-6, and (*ii*) a stress-reduction regressive rarefaction front propagates from particle-6 towards particle-1 (Fig. 9). The rarefaction front initiated at particle-6 arrives at particle-5 faster than the compression front, particle-5 looses support, and particle flow is triggered in the vicinity of particle-5. The contact force does not need to reach zero, but rather to reduce to a point where equilibrium is compromised due to slippage. It is anticipated that the acceleration required for destabilization increases with increasing skeletal forces in the particles forming the bridge. These forces may be induced by drag forces when fluids flow through, which explains the higher stability exhibited when bridges are subjected to high fluid velocity (Muecke 1979). On the other hand, large drag forces may actually destabilize asymmetric bridges (Bratli and Risnes 1981; Valdes 2002). This situation is exacerbated in bridges made of a large number of particles n – Fig. 7).

Experimental results in Fig. 8 suggest that high acceleration levels (i.e., a equal to 10 to 50 m/s^2) are needed to cause bridge destabilization. These may be difficult to attain in practical applications: the combination of geometric spreading and the increased attenuation with wave propagation frequency. Although frequency f affects acceleration by f^2, attenuation in granular materials increases with increasing frequency. Hence, the implementation of vibration-based unclogging would require the placement of the vibration source close to the potential clogging location.

Conclusions

Flowing particles can form bridges at pore throats. This pore-scale mechanism is relevant to filter clogging and unclogging, water and oil extraction, sand production in oil wells, and to food grain, aggregate, and powder handling operations.

Fig. 8. Vibration-based bridge destabilization. Tripartite plots for two different test procedures. Tests are conducted with d_o/d = 4.15 for glass beads, d_o/d = 4.5 for sand particles, and d_o/d = 5.5 for mica flakes (d = 1 mm for mica; Table 1).

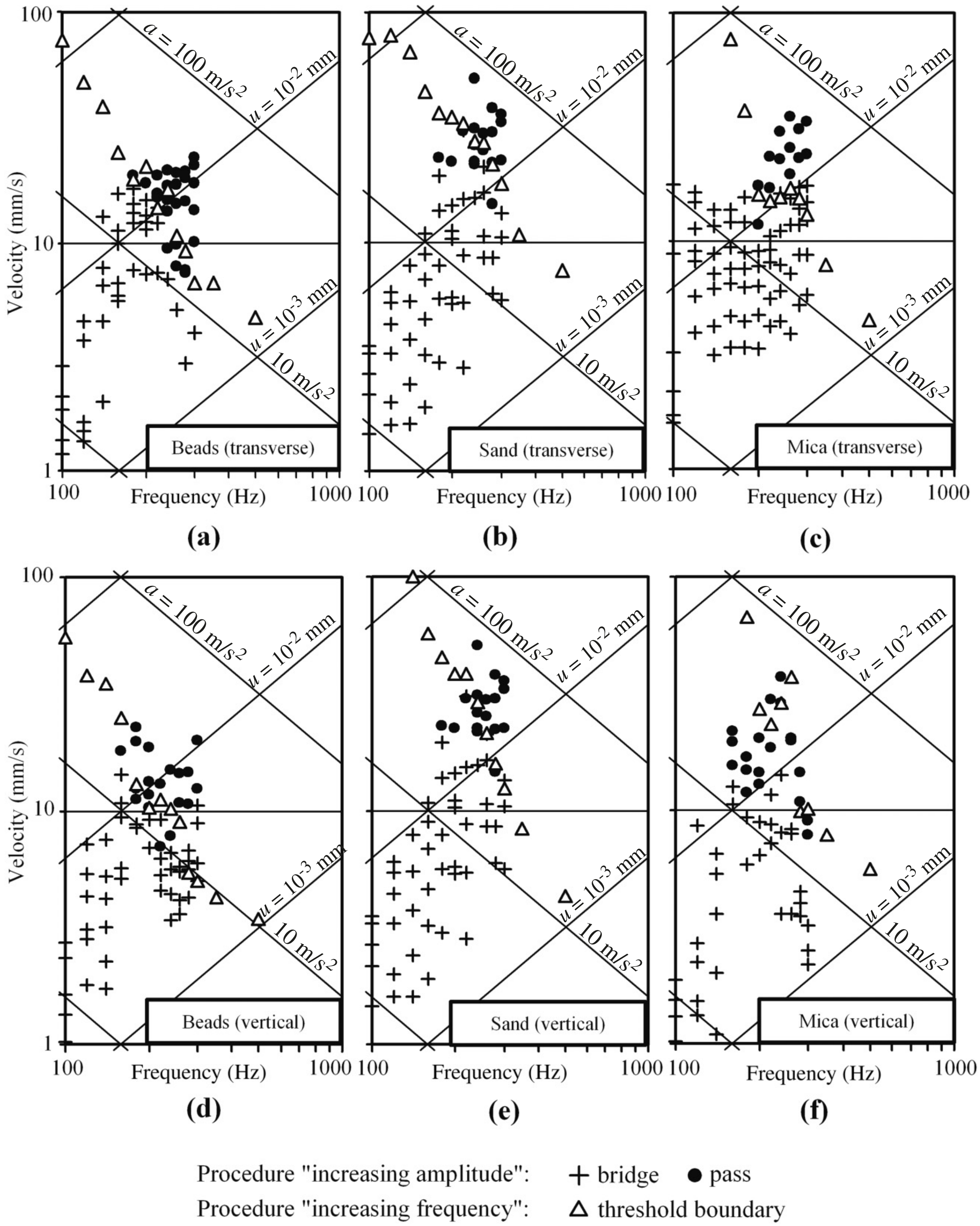

Results from this study show that the stability of a particulate bridge depends on the geometric characteristics of the bridge-forming particles (sphericity, platiness, and roughness) and the distribution of force chains within the bridge. Particle shape affects bridge formation considerably: smooth spherical glass beads particles form smaller stable bridges than the rougher and less spherical Ottawa sand particles. Furthermore, flat particles can span orifices with the greatest d_o/d ratios. Particle orientations in flat particle bridges are dependent on d_o/d.

Three regimes are identified in terms of the relative size ratio d_o/d. On one extreme, bridges are stable even under vibration (e.g., $d_o/d < \delta_{min}$ ~3 to 4 for Ottawa sand). At the other extreme, bridges never form and continuous granular flow is observed (e.g., $d_o/d \geq \delta_{max}$ ~5 for Ottawa sand). Bridge formation is vibration sensitive between these two regimes.

Vibration promotes the transport of migratory particles by destabilizing existing bridges and by preventing successive bridge formation. Experimental evidence highlights the importance of acceleration in bridge destabilization, (i.e., iner-

Fig. 9. Bridge collapse due to the sudden movement of the supporting plate (retraced from high-speed digital images). Destabilization movements start on the far side of the orifice with respect to the applied disturbance and results from the bridge's inability to sustain a back-propagating rarefaction front.

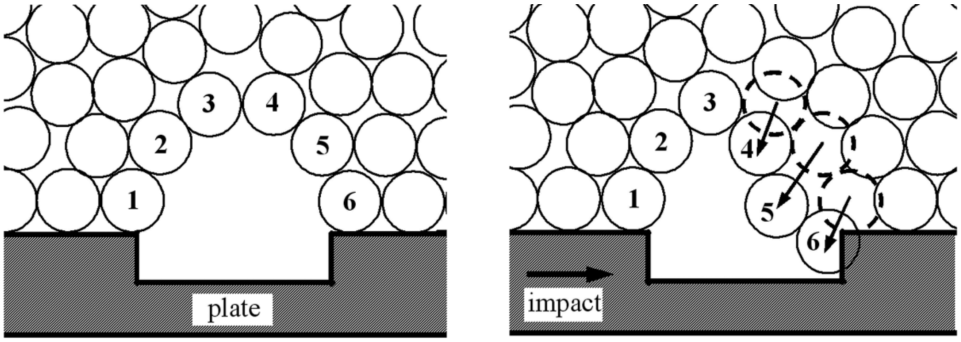

tial forces). Furthermore, results suggest that it is easier to prevent bridge formation than to destabilize formed bridges. Vibration is most effective for smooth spherical particles and for flat particles that span large throats. Bridges made of rougher particles and with small d_o/d ratios are less susceptible to vibrations, and in general, higher accelerations are needed to cause their destabilization. High accelerations and frequencies needed for bridge destabilization translate to challenges in applying vibration methods in large field applications.

Microscale experimental studies performed with circular disks suggest that vibration-based bridge destabilization is controlled by the inability of the bridge to transfer a rarefaction front or by the presence of irregularities in the bridge geometry.

Acknowledgements

Support for this research was provided by the Goizueta Foundation, Shell, and the US National Science Foundation.

References

Bertram, G.E. 1940. Experimental investigation of protective filters. Soil Mechanics Series 7, Harvard University, Cambridge Mass.

Bigno, Y., Oyeneyin, M.B., and Peden, J.M. 1994. Investigation of pore-blocking mechanism in gravel packs in the management and control of fines migration. *In* Proceedings of Society of Petroleum Engineers International Symposium on Damage Control, Lafayette, La., 9–10 February 1994. Society of Petroleum Engineers (SPE), Richardson, Tex. pp. 29–40.

Bratli, R.K., and Risnes, R. 1981. Stability and failure of sand arches. Society of Petroleum Engineers Journal, **21**(2): 236–248.

Gruesbeck, C., and Collins, E. 1982. Particle transport through perforations. Society of Petroleum Engineers Journal, **22**(6): 857–865.

Ives, K.J. 1980. Deep bed filtration: theory and practice. Filtration and Separation, **17**(2): 157–168.

Kenney, T.C., Chahal, R., Chiu, E., Ofoegbu, G.I., Omange, G.N., and Ume, C.A. 1985. Controlling constriction sizes of granular filters. Canadian Geotechnical Journal, **22**(1): 32–43. doi:10.1139/t85-005.

Krumbein, W.C., and Sloss, L.L. 1963. Stratigraphy and sedimentation. 2nd ed. W.H. Freeman and Company, San Francisco, Calif.

McDowell-Boyer, L.M., Hunt, J.R., and Sitar, N. 1986. Particle transport through porous media. Water Research, **22**(13): 1901–1921. doi:10.1029/WR022i013p01901.

Muecke, T.W. 1979. Formation fines and factors controlling their movement in porous media. Journal of Petroleum Technology, **31**(1): 144–150. doi:10.2118/7007-PA.

Ramachandran, V., and Fogler, H.S. 1999. Plugging by hydrodynamic bridging during flow of stable colloidal particles within cylindrical pores. Journal of Fluid Mechanics, **385**: 129–156. doi:10.1017/S0022112098004121.

Sakthivadivel, R., and Einstein, H.A. 1970. Clogging of porous column of spheres by sediment. ASCE Journal of Hydraulics Engineering, **96**(2): 461–472.

Sherard, J.L., Dunnigan, L.P., and Talbot, J.R. 1984. Basic properties of sand and gravel filters. Journal of Geotechnical Engineering, **110**(6): 684–701.

U.S. Corps of Engineers, Waterways Experiment Station WES. 1953. Filter experiments and design criteria. Technical Memorandum 3–360. Vicksburg, Miss.

Valdes, J.R. 2002. Fines migration and formation damage – microscale dtudies. Ph.D. dissertation, Georgia Institute of Technology, Atlanta, Ga.

Valdes, J.R., and Santamarina, J.C. 2006. Particle clogging in radial flow: microscale mechanisms. Society of Petroleum Engineers Journal, **11**(2): 193–198.

Watson, P.D.J., and John, N.W.M. 1999. Geotextile filter design and simulated bridge formation at the soil-geotextile interface. Geotextiles and Geomembranes, **17**: 265–280. doi:10.1016/S0266-1144(99)00013-8.

List of symbols

a	acceleration
C_u	coefficient of uniformity
d	migratory particle diameter
d_{10}	particle size: 10th percentile (by mass)
d_{50}	mean particle size: 50th percentile (by mass)
d_{60}	particle size: 60th percentile (by mass)
d_o	throat diameter
D	filter matrix particle diameter
f	frequency
G_s	specific gravity
n	number of particles
R	radius of a circle; roundness
S	sphericity
u	displacement
v	velocity
β	size ratio
φ_d	dilatancy angle at base of bridge
δ	critical size ratio d_o/d describing bridging regimes
δ_{min}	size ratio d_o/d below which stable bridges are formed
δ_{max}	size ratio d_o/d above which no bridges are formed
γ	angle between adjacent particles in a bridge